

Leading Quenching Effects in the Proton Magnetic Moment

R. D. Young,¹ D. B. Leinweber,¹ and A. W. Thomas^{1,2}

¹ *Special Research Centre for the Subatomic Structure of Matter,
and Department of Physics and Mathematical Physics,
University of Adelaide, Adelaide SA 5005, Australia*

² *Jefferson Laboratory, 12000 Jefferson Ave., Newport News, VA 23606 USA*

We present the first investigation of the extrapolation of quenched nucleon magnetic moments in quenched chiral effective field theory. We utilize established techniques in finite-range regularisation and compare with standard dimensional regularisation methods. Finite-volume corrections to the relevant loop integrals are also addressed. Finally, the contributions of dynamical sea quarks to the proton moment are estimated using a recently discovered phenomenological link between quenched and physical QCD.

I. INTRODUCTION

Describing the quark content of nucleon structure in terms of QCD is a fundamental aim of modern nuclear physics. As an inherently nonperturbative theory, the most rigorous approach to low-energy phenomena in QCD is by numerical simulations in lattice gauge theory. Although restricted at present to the regime of quark masses exceeding those realized in nature, recent advances in effective field theory (EFT) have made it possible to accurately extract the physical nucleon mass from QCD [1].

These advances and breakthroughs in chiral effective field theory (χ EFT) have their origin in the study of a range of hadron properties in QCD, including nucleon magnetic moments and charge radii [2, 3, 4, 5], the nucleon sigma commutator [1, 6, 7], moments of structure functions [8, 9, 10] and the ρ -meson mass [11].

With the the most detailed studies being on the extrapolation of the nucleon mass, it has been shown that the use of finite-range regularisation (FRR) enables the most systematically accurate connection of effective field theory and lattice simulation results [1, 12, 13]. Mathematically equivalent to dimensional regularisation (DR) to any finite order, FRR chiral effective field theory provides a resummation of the chiral expansion with vastly improved convergence properties. Central to FRR is the presence of a finite energy scale which may be used to optimize the convergence properties of the truncated expansion. The success of FRR-EFT is highlighted by the observation that the higher-order terms of the traditional dimensionally regulated expansion, although individually large, must sum to zero to describe lattice QCD results.

Here FRR- χ EFT is applied to nucleon magnetic moments calculated in lattice QCD. In particular, we investigate the modifications required for the extrapolation of quenched simulation results. Issues with the formulation of EFT on a finite volume are also discussed. We consider the modifications to chiral loop integrals on a finite volume and perform a fixed-volume extrapolation.

We extend a phenomenological link between quenched and dynamical baryon masses [14] to the case of magnetic moments to estimate the artifacts associated with

the quenched approximation. We find that the full QCD corrections of the quenched magnetic moments are small over a wide range of quark mass.

Finally, the convergence properties of a truncated Taylor-series expansion of the FRR results in powers of m_π , analogous to that encountered in dimensional regularisation, are investigated. We illustrate how any moderate truncation of the series expansion is unable to connect with current lattice simulation results. The inclusion of higher-order chiral loop corrections associated with the Δ baryon are also considered and found to be small.

II. MAGNETIC MOMENTS — QUARK MASS DEPENDENCE

In a general construction of an effective field theory for low-energy QCD, the expansion of the nucleon's magnetic moment about the chiral limit can be written as

$$\mu_B = a_0^B + a_2^B m_\pi^2 + a_4^B m_\pi^4 + \dots + \chi_{B\pi} I_\pi + \dots \quad (1)$$

The term $\chi_{B\pi} I_\pi$ denotes the leading nonanalytic (LNA) chiral correction to the baryon magnetic moment of Fig. 1. Coefficients of low-order nonanalytic contributions to nucleon properties are determined model-independently and are known to high precision phenomenologically [15]. For example, the LNA coefficient to the proton magnetic moment is given by

$$\chi_{p\pi} = -\frac{g_A^2 M_N}{8\pi f_\pi^2}. \quad (2)$$

Any extrapolation of lattice QCD simulations must incorporate this knowledge of QCD.

The analytic terms are unconstrained by chiral symmetry, and hence must be determined empirically. Lattice QCD provides an *ab initio* framework to determine these parameters from QCD.

The expression, Eq. (1), is analogous to the chiral expansion of the nucleon mass described in Refs. [1, 12]. The regulator dependence of the integrals is implicit.

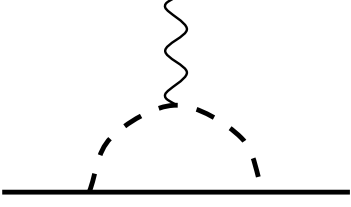


FIG. 1: Diagram providing the leading non-analytic contribution of pions (dashed curve) to the nucleon (solid line) magnetic moment.

To define the expansion one must define a regularisation and renormalisation scheme to remove ultra-violet divergences.

In the text-book approach to elementary field theory one commonly uses dimensional regularisation to renormalise the theory. In this case, only the residue of the pion pole becomes apparent and the loop contribution is therefore given by

$$\chi_B I_\pi^{\text{DR}} \rightarrow \chi_B m_\pi, \quad (3)$$

and the linear divergence of the integral is absorbed into an infinite renormalisation of a_0 .

Alternatively, ultra-violet divergences can be removed by suppressing loop integrals above a finite energy scale. The first systematic study of finite-range regularisation in χ PT was performed by Donoghue et al. [16]. The development of FRR- χ PT in the context of lattice QCD [1, 11, 12, 13, 14, 17] has found remarkably improved convergence properties of the chiral expansion, providing access to a much wider range of range of quark mass than the naively regularised theory [12]. FRR is therefore best suited to the problem of chiral extrapolation, where the systematic error in the extrapolation of modern lattice simulations is of order 1% [1].

Using FRR, the loop integral, I_π , in the heavy baryon limit can be expressed as

$$I_\pi = -\frac{4}{3\pi} \int dk \frac{k^4 u^2(k)}{\omega_k^4}, \quad (4)$$

where $\omega_k = \sqrt{k^2 + m_\pi^2}$ and $u(k)$ is the ultra-violet regulator.

Expansion of the loop contributions as a power series enables one to obtain the renormalised chiral expansion parameters, where each of the analytic terms in Eq. (1) are renormalised by a finite amount [12, 16]. For example, using a dipole regulator, $u(k) = (1 + k^2/\Lambda^2)^{-2}$, Eq. (4) becomes

$$I_\pi^{\text{DIP}} = -\frac{\Lambda^5(m_\pi + 5\Lambda)}{24(m_\pi + \Lambda)^5}, \quad (5)$$

and the Taylor expansion provides

$$I_\pi^{\text{DIP}} = -\frac{5}{24}\Lambda + m_\pi - \frac{35}{12\Lambda}m_\pi^2 + \dots \quad (6)$$

Therefore, precisely the same LNA contribution is recovered

$$\chi_{B\pi} I_\pi^{\text{DIP (LNA)}} = \chi_{B\pi} m_\pi, \quad (7)$$

with a finite renormalisation of all other terms in the series. By varying Λ , strength in the loop integral may be moved to the residual analytic expansion and vice-versa. As the moderately large m_π behaviour of the loop integral and the residual expansion are radically different, varying Λ provides an opportunity to optimize the convergence properties of the truncated chiral expansion.

We show the mathematical equivalence of the renormalisation prescriptions to a given order. The renormalised expansion in dimensional regularisation is

$$\mu_B = c_0^B + \chi_{B\pi} m_\pi + c_2^B m_\pi^2 + \dots, \quad (8)$$

and these renormalised coefficients are recovered from the FRR expansion via

$$\begin{aligned} c_0^B &= a_0^B - \chi_{B\pi} \frac{5}{24}\Lambda, \\ c_2^B &= a_2^B - \chi_{B\pi} \frac{35}{12\Lambda}, \end{aligned} \quad (9)$$

where the second terms compensate the Λ dependence of a_i^B .

In summary, in working to leading order in the chiral expansion with a dipole FRR, the quark mass dependence of nucleon magnetic moments in QCD is

$$\mu_B = a_0^B + a_2^B m_\pi^2 + a_4^B m_\pi^4 - \chi_{B\pi} \frac{\Lambda^5(m_\pi + 5\Lambda)}{24(m_\pi + \Lambda)^5}. \quad (10)$$

The inclusion of an m_π^4 term here is in anticipation of adding NLNA terms in the following.

III. QUENCHED CONSIDERATIONS

Here we address the necessary modifications to the chiral effective field theory for the quenched approximation. Vacuum fluctuations of $q\bar{q}$ -pairs are absent in quenched simulations. As a result, the structure of the low-energy effective field theory is modified. Meson loop diagrams are restricted to only those where the loop is comprised of valence quarks having their origin in the interpolating fields of the baryon correlation function. This has the effect of modifying the effective π - N coupling constants [18, 19] and the corresponding factors χ_B are changed accordingly.

To summarize the LNA contributions to nucleon magnetic moments in both quenched and dynamical QCD, we use the standard notation and define

$$\chi_{B\pi} = \frac{M_N}{8\pi f_\pi^2} \beta_B^\pi, \quad (11)$$

and provide the coefficients, β_B^π , are in Table I [18, 19]. We use $f_\pi = 93$ MeV, $D = 0.76$ and $F = 0.50$, ($g_A = D + F$).

TABLE I: Coefficients of the leading pion-loop contributions to nucleon magnetic moments in QCD and QQCD.

Baryon	β_B^π	$\beta_B^{\pi(Q)}$
p	$-(F + D)^2$	$-\frac{4}{3}D^2$
n	$(F + D)^2$	$\frac{4}{3}D^2$

A peculiar feature of the quenched theory is the appearance of the flavour-singlet η' -meson as a light degree of freedom. In the absence of vacuum quark loops the η' behaves as a Goldstone boson [20, 21] and must therefore be incorporated in the low-energy effective field theory.

The η' carries no charge and therefore does not make a direct contribution to the magnetic moment of the nucleon. The leading enhancement of the moment comes from η' -dressing of the current insertion as in Fig. 2. Being a flavour singlet, the η' can propagate through a pure gluonic state. This corresponds to a double-hairpin in the quark-flow diagram. The vertex correction to the magnetic moment induced by this loop produces more singular nonanalytic behaviour in the chiral limit than the physical theory.

The double-hairpin diagram has a logarithmic divergence near the chiral limit. This is a pathological feature of the quenched approximation, where the magnetic moment tends to infinity near the chiral limit. Physically this is not possible as angular momentum quantization ensures that the induced magnetic field of the meson-loop remains finite, even in the chiral limit [22].

The double-hairpin vertex correction diagram has been calculated in the graded-symmetry approach to Q χ PT by Savage in Ref. [18], and provides the term

$$\chi_{\eta'}^{(Q)} \mu_B^{(Q)\text{tree}} I_{\eta'}, \quad (12)$$

with coefficient

$$\chi_{\eta'}^{(Q)} = \frac{m_0^2 (3F - D)^2}{12 \pi^2 f_\pi^2}. \quad (13)$$

The superscript (Q) denotes a quenched quantity. The coefficient m_0^2 is associated with the double-hairpin vertex in the η' propagator. This parameter is related to

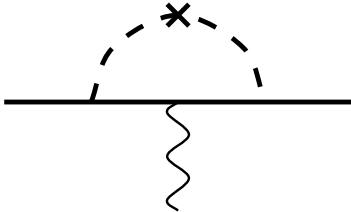


FIG. 2: Double-hairpin η' vertex correction to nucleon magnetic moment.

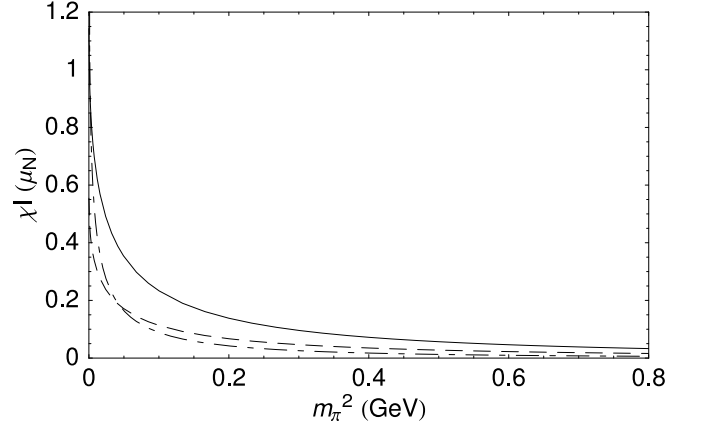


FIG. 3: Loop corrections, in units of μ_N , evaluated with a dipole FRR with $\Lambda = 0.8$ GeV. The dashed and solid curves are the pion loop corrections of Fig. 1 in quenched and physical QCD respectively. The dash-dot curve is the η' vertex correction of quenched QCD, where the physical magnetic moment is used to define the renormalized coupling.

the physical η' mass [20, 21] and we choose a value $m_0^2 = 0.42$ GeV. The loop integral in the heavy-baryon limit is given by

$$I_{\eta'} = - \int dk \frac{k^4 u^2(k)}{\omega_k^5}. \quad (14)$$

The normalization of the integral is such that the LNA contribution to this loop is $\log m_\pi$.

We also highlight that this contribution is proportional to the tree-level moment, $\mu_B^{(Q)\text{tree}}$ [18]. Because of the logarithmic divergence one cannot simply define this to be the renormalised moment in the chiral limit. This necessarily means that one cannot remove the scale dependence of the coefficient of this chiral log using standard methods. We remove the scale dependence by replacing the tree level coefficient by the renormalised magnetic moment at each quark mass $\mu_B^{(Q)\text{tree}} = \mu_B^{(Q)}$. This approximation will be accurate provided $\chi_{\eta'}^{(Q)} \mu_B^{(Q)\text{tree}} I_{\eta'}$ makes only small contributions for $m_\pi > m_\pi^{\text{phys}}$.

In Figure 3 we show the value of the loop contributions for varying pion mass. The corrections from the η' are quite small in the region of interest.

Our expansion in the quenched approximation, analogous to Eq. (1), is given by

$$\begin{aligned} \mu_B^{(Q)} &= a_0^{B(Q)} + a_2^{B(Q)} m_\pi^2 + a_4^{B(Q)} m_\pi^4 \\ &\quad + \chi_{B\pi}^{(Q)} I_\pi + \chi_{B\eta'}^{(Q)} \mu_B^{(Q)} I_{\eta'}, \end{aligned} \quad (15)$$

and is used to determine the parameters $a_i^{B(Q)}$. The total magnetic moment at arbitrary m_π is then given by

$$\begin{aligned} \mu_B^{(Q)} &= \left\{ a_0^{B(Q)} + a_2^{B(Q)} m_\pi^2 + a_4^{B(Q)} m_\pi^4 \right. \\ &\quad \left. + \chi_{B\pi}^{(Q)} I_\pi \right\} \left(1 - \chi_{B\eta'}^{(Q)} I_{\eta'} \right)^{-1}. \end{aligned} \quad (16)$$

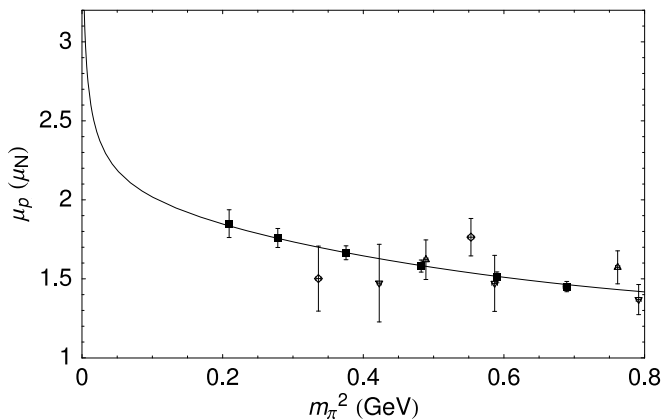


FIG. 4: Fit of Eq. (15) to quenched lattice data. The solid squares (■) illustrate the FLIC fermion results [24, 25] and the open symbols describe nonperturbatively improved clover results [23], at $\beta = 6.0$ (∇), $\beta = 6.2$ (\triangle) and $\beta = 6.4$ (\diamond).

We note that at this point the decuplet contributions have been suppressed as their contributions are higher-order in the chiral expansion, when one accounts for the octet-decuplet mass splitting realized in the (quenched) chiral limit [14].

IV. EXTRAPOLATION OF LATTICE MAGNETIC MOMENTS

With the expansion of the low-energy EFT determined, one needs to fix the values of the unconstrained terms empirically. Lattice QCD provides information on the quark mass dependence of hadronic properties and hence enables the determination of these free parameters. If the data analyzed is within the applicable range of the effective field theory then, upon fixing these low-energy constants, one has an accurate extrapolation to the physical regime.

The electromagnetic form factors of the nucleon have recently been studied in simulations of quenched lattice QCD [23, 24, 25]. Early simulations of nucleon three-point functions have been performed by Leinweber *et al.* in Ref. [26]. Direct lattice calculations of the nucleon's strangeness form factor have also been carried out in Refs. [27, 28].

In this study we choose to analyze only the most recently performed simulations using improved quark actions. Results by Gockeler *et al.* [23] have been obtained using the nonperturbatively improved clover fermion action [29]. We also consider recent form factor simulations by Zanotti *et al.* [24, 25] using the fat-link irrelevant clover (FLIC) quark action [30]. For the purposes of this investigation, we select the six most accurate data points from the FLIC data set. The precision of the FLIC fermion results reflects the use of improved unbiased estimation techniques [26], improved actions and high statis-

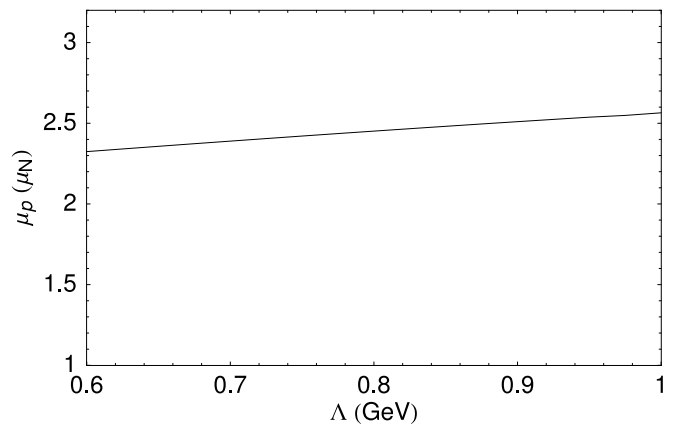


FIG. 5: The dependence of the extrapolated magnetic moment determined at the physical pion mass on the dipole regulator parameter Λ . Variation in the quenched proton moment is similar to the statistical uncertainty of the FLIC simulation result at the lightest quark mass considered.

tics. It has been demonstrated that FRR- χ EFT is applicable up to $m_\pi^2 = 0.8 \text{ GeV}^2$ [12] and hence we also choose to truncate our data set at this scale of pion mass.

All previous chiral extrapolations of lattice electromagnetic structure have been based on χ PT under the assumption that quenching effects are minimal [2, 3, 4, 5, 17, 23, 31, 32, 33]. Here we present the first comprehensive analysis of quenched lattice magnetic moments using $Q\chi$ PT for baryon form factors. Brief reports on preliminary $Q\chi$ PT extrapolations have recently been presented in Refs. [34, 35, 36].

In Fig. 4 we show fits to quenched lattice data of the proton magnetic moment using Eqs. (15) and (16). In anticipation of estimating unquenching corrections we have adopted the preferred value of $\Lambda = 0.8 \text{ GeV}$ [14]. The logarithmic divergence of μ_p in the chiral limit is evident.

Fig. 5 illustrates the dependence of the extrapolated result, evaluated at the physical pion mass, on the choice of regulator parameter Λ . The vertical axis has been fixed to that of Fig. 4 in order to display the relevant scale. The variation in the quenched proton moment is similar to the statistical uncertainty of the FLIC simulation result at the lightest quark mass considered. Further reduction of the Λ sensitivity could be obtained by considering higher-order terms of the chiral expansion.

V. EXTRAPOLATION ON A FINITE VOLUME

The previous section assumed the lattice QCD results provide an accurate representation of the results to be realized in the infinite-volume limit. However, results obtained on a lattice of finite spatial extent will differ from those in the infinite volume limit, particularly in the chiral regime where the pion Compton wavelength can approach the lattice length. Here we extend the for-

malism of FRR to incorporate finite-volume effects.

The leading-order finite-volume effect in the chiral expansion lies in terms analytic in the small expansion parameter, $1/L$, where L is the length of the cubic volume [37]. Finite-volume corrections also enter through the modification of loop integrals. The requirement that Greens functions are periodic [37] restricts momentum components to the values

$$k_i = \frac{2\pi n_i}{L}, \quad n_i = 0, \pm 1, \pm 2, \dots \quad (17)$$

For the p -wave loop contribution of Fig. 1, where strength in the integrand vanishes for $k = 0$ as in Eq. (4), the dominant effect of discretizing the momenta is to introduce a threshold effect [11, 14]. Strength in the integrand is not sampled until one component of k reaches $2\pi/L$. Since chiral physics is dominated by the infrared behaviour of loop integrals, the nonanalytic terms of the chiral expansion exhibit substantial threshold effects.

To obtain a complete description of the quark mass and volume dependence of hadron properties, one must have an expansion in both m_q and $1/L$ [37]. Without data at varying lattice volumes it is impossible to determine the coefficients of the $1/L$ terms which dominate the finite volume corrections in the chiral regime. Recent estimates [38, 39] of finite volume corrections in lattice QCD simulations have neglected the $1/L$ terms and, using dimensional-regularization related techniques, predict finite volume corrections which vanish in the chiral limit. Such formulations predict volume corrections which grow with pion mass, in disagreement with very general physical arguments. However, impressive results for a phenomenological description of the volume dependence of hadron masses, which are suppressed for larger pion mass, have recently been reported [40].

In the absence of lattice QCD results for magnetic moments from a variety of lattice volumes, it is not possible to rigorously constrain the complete volume-dependent expansion. However, it is possible to precisely describe the impact of the finite volume on the quark-mass dependence of magnetic moments on a single, fixed lattice volume.

Evaluating the loop integrals on a finite volume in FRR is a rather simple extension. One simply replaces the continuum integral by the discrete momentum sum over available momenta on a given volume. We formulate the finite-volume corrections in the continuum theory and therefore continue the momentum sum to infinity. This allows the features of finite-range regularization to carry over to the finite volume case. For example, Eq. (4) becomes

$$\begin{aligned} I_\pi &= -\frac{4}{3\pi} \int dk \frac{k^4 u^2(k)}{\omega_k^4} = -\frac{1}{3\pi^2} \int d^3k \frac{k^2 u^2(k)}{\omega_k^4} \\ &\rightarrow -\frac{1}{3\pi^2} \left(\frac{2\pi}{L}\right)^3 \sum_{\vec{k}} \frac{k^2 u^2(k)}{\omega_k^4}. \end{aligned} \quad (18)$$

The discretized momenta on a cube are given by $\vec{k} =$

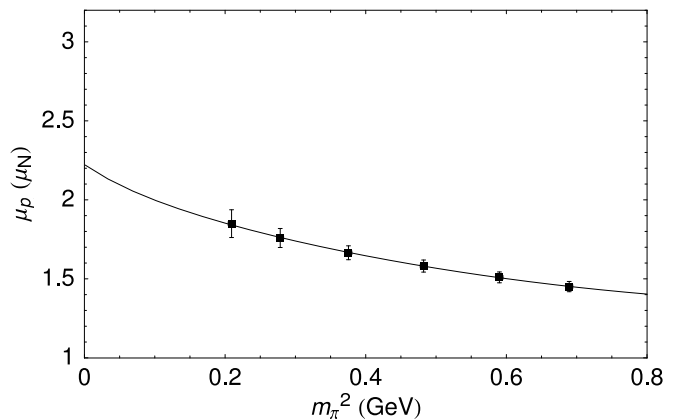


FIG. 6: Finite-volume FRR-EFT fit to FLIC fermion results for fixed volume. Here the dipole-vertex regulator parameter is fixed to $\Lambda = 0.8$ GeV.

$k_{\min} \vec{n}$ for $\vec{n} \in \mathbb{Z}^3$, with the minimum nontrivial momentum given by $k_{\min} = 2\pi/L$. We note that in obtaining the infinite volume form of Eq. (4) the angular dependence of the 3-dimensional integral has been performed analytically. In general, with an angular dependent integrand, one must take caution in the naive conversion to a spherically symmetric sum as shown in Eq. (18). For the integrals used in this paper, we have verified that the spherically symmetric and angular dependent summations are equivalent.

Simulations performed with standard Wilson actions have large $\mathcal{O}(a)$ errors that can be accounted for in the effective field theory. One can introduce new local operators into the chiral Lagrangian reflecting $\mathcal{O}(a)$ terms associated with lattice discretization effects and explicit chiral symmetry breaking [41, 42, 43]. However, there has been tremendous success in removing $\mathcal{O}(a)$ errors and suppressing $\mathcal{O}(a^2)$ errors in lattice simulation results through the development of nonperturbatively improved actions [30, 44, 45]. These actions display excellent scaling properties [46, 47, 48], providing near continuum results at finite lattice spacing. In particular, the FLIC fermion simulations, dominating the chiral fits here, are performed using an $\mathcal{O}(a^2)$ -mean-field improved Luscher-Weisz plaquette plus rectangle gauge action [49] and the nonperturbatively $\mathcal{O}(a)$ -improved FLIC fermion action [30, 46]. Hence these lattice results already represent an excellent approximation to the continuum limit.

Fig. 6 illustrates the fit of Eq. (15) with the π and η' loop integrals modified as described in Eq. (18) for the finite volume. The physical volume of the FLIC lattice is $V = (2.56 \text{ fm})^3$. The chiral properties of the finite-volume extrapolation are qualitatively different from the infinite volume curve of Fig. 4. In Fig. 7 we show the regulator parameter dependence on the finite-volume extrapolated magnetic moment for Λ in the range 0.6–1.0 GeV. The variation of the extrapolated moment is suppressed relative to the infinite volume case, changing

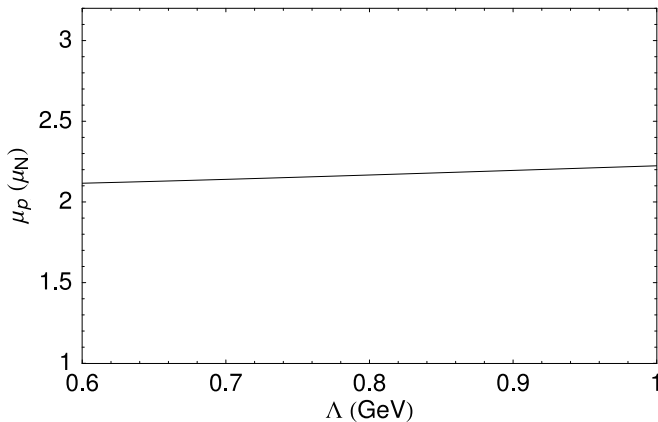


FIG. 7: The extrapolated magnetic moment on a finite volume, $V = (2.56 \text{ fm})^3$, for varying regulator parameter Λ .

by $0.1 \mu_N$. This systematic uncertainty is smaller than the statistical uncertainty of the lightest quark mass considered here, and could be suppressed further through the introduction of higher-order terms in the chiral expansion or through the introduction of precise lattice QCD results at light quark masses.

VI. ESTIMATING EFFECTS OF DYNAMICAL SEA QUARKS

In a study of baryon masses in quenched and 2+1-flavour QCD it has been found that the short-distance physics of the analytic terms in the residual expansion of FRR-EFT are found to be very similar when the chiral-loop effects are evaluated with an appropriate FRR [14]. By identifying the short distance behaviour in QQCD, one need only restore the chiral loop effects of QCD to obtain an improved estimate of the physical magnetic moment.

In making such an identification it is essential to have a consistent method for setting the scale in both quenched and dynamical QCD. In particular, one must ensure that the procedure is insensitive to chiral physics. The QCD Sommer scale [50], based on the static quark potential, is insensitive to light quark physics and provides an ideal procedure for the scale determination.

The identification of this phenomenological link between quenched and dynamical simulations has been applied to FLIC fermion calculations of baryon masses [34, 36]. Upon replacing the chiral loops of QQCD by their QCD counterparts the nucleon and Delta are found to be in good agreement with experiment.

By applying the same principle to the calculation of magnetic moments in quenched QCD one can obtain improved estimates of the physical magnetic moment. The fit parameters, $a_i^{B(Q)}$, are determined by fitting finite-volume quenched lattice QCD using Eq. (15) with discretized momenta and a dipole regulator of 0.8 GeV.

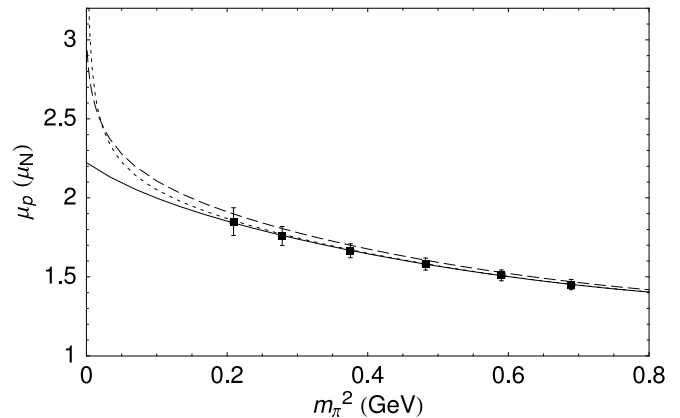


FIG. 8: Correcting the finite-volume quenched approximation to the infinite-volume limit of full QCD. The solid curve is the finite-volume quenched fit to the data as in Fig. 4. The dotted curve provides an estimate of the infinite-volume limit magnetic moment in the quenched approximation. The dashed curve shows estimates of the proton magnetic moment in full QCD as described in the text.

The estimate of the quenching effects are obtained under the assumption that the bare residual expansion parameters are unchanged in infinite-volume QCD when $\Lambda = 0.8 \text{ GeV}$. That is, the full QCD result can be described by Eq. (10) with the identification $a_i^{B(Q)} = a_i^B$. By fitting with finite-volume FRR-EFT both quenching and finite-volume corrections are incorporated in the final estimate. We show the infinite-volume QCD estimate of the proton magnetic moment by the dashed curve in Fig. 8.

In a similar manner, the infinite-volume limit of QQCD is estimated by fitting the parameters $a_i^{B(Q)}$ of Eq. (15) using finite-volume discretized momenta and a dipole regulator of 0.8 GeV in the loop integrals. The correction is estimated by Eq. (16) calculated with infinite-volume continuous momenta in the loop integrals. Figure 8 illustrates that the finite volume corrections are negligible in the regime of the lattice QCD simulation results.

We emphasize that this result is a phenomenological estimate, as the size of the correction is Λ dependent. However an important feature of this approach is that the largest finite volume corrections lie in the chiral limit as they should. Ultimately, one would like to combine the improved convergence properties of FRR-EFT with the small $1/L$ expansion such that accurate and model-independent determinations of finite volume effects can be made.

The primary feature of Fig. 8 is that although the quenched and physical theory have quite different chiral structure, the observable effects are quite small. In particular, the logarithmic divergence is likely to only become apparent well below the physical pion mass. Within the current formalism of lattice QCD it seems such observation would be a formidable task, particularly given the

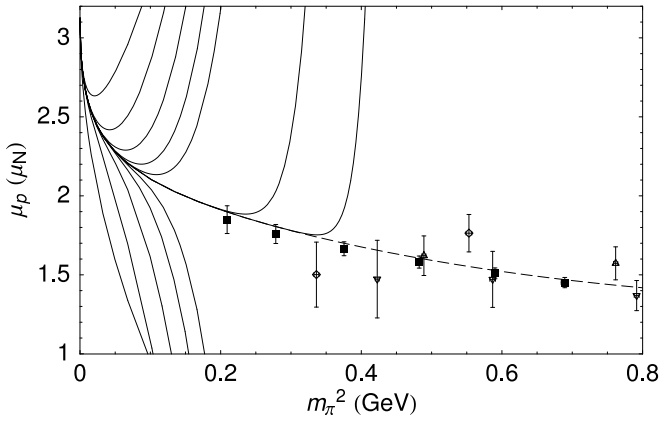


FIG. 9: Truncations of the Taylor expansion of the full QCD expression of the magnetic moment, Eq. (10), to various orders in m_π . The left most curves display a succession of truncations from m_π up to m_π^{10} . To reach convergence at the lightest FLIC data point considered here one requires terms up to m_π^{26} , while for QCDSF terms to m_π^{50} are necessary. The dashed curve displays the full QCD expression as displayed in Fig. 8.

large finite volume required to reveal the η' contribution.

The results here, based on the leading chiral corrections, indicate that proton magnetic moments evaluated in quenched simulations give a good approximation to the true theory. The enhancement from the η' -loop compensates for the reduction in the standard pion-loop from QCD to QQCD. The similarity in the effective curvature was also highlighted by Savage [18].

VII. SERIES TRUNCATION AND HIGHER ORDER EFFECTS

It is interesting to explore the convergence properties of the series expansion, generated in dimensional regularisation, truncated to various order in m_π . Information on the convergence of the truncated series can be obtained by studying the Taylor series expansion of the FRR dipole regularised form, Eq. (10), which describes lattice results very well. Determination of the convergence of the series will therefore give insight into the applicable range of a dimensionally regularised expansion. Similar studies of a truncation of the chiral loop corrections to the nucleon mass evaluated with a FRR have been performed in Refs. [51, 52, 53].

In Fig. 9 we show the Taylor series expansion of Eq. (10) truncated at various powers of m_π . This plot indicates that in order to accurately reproduce the quark mass dependence of the proton magnetic moment up to $m_\pi \sim 0.1 \text{ GeV}^2$ then one must keep all terms up to m_π^{10} , *i.e.* m_q^5 . If one wishes to reach the quark mass scale of modern lattice QCD simulations many more powers in m_π are required. In fact, the lightest displayed FLIC quark mass requires terms to m_π^{26} , similarly the lightest

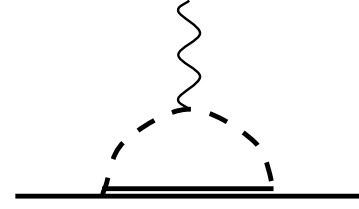


FIG. 10: Leading pion-loop contribution to nucleon magnetic moment from the Δ resonance.

TABLE II: Coefficients of the leading decuplet, pion-loop contributions to nucleon magnetic moments in QCD and QQCD [18], $\mathcal{C} = -2D$.

Baryon	$\beta_{B\Delta}^\pi$	$\beta_{B\Delta}^{\pi(Q)}$
p	$-\frac{2}{9}\mathcal{C}^2$	$-\frac{1}{6}\mathcal{C}^2$
n	$\frac{2}{9}\mathcal{C}^2$	$\frac{1}{6}\mathcal{C}^2$

QCDSF point needs m_π^{50} .

This problem might have been anticipated by the fact that at moderately large quark masses the Dirac moment of the nucleon would be revealed

$$\mu_p = \frac{e\hbar}{2M_N}. \quad (19)$$

Knowing that in this regime, the nucleon mass grows linearly with m_π^2 , the moment would require an expansion in inverse powers of m_π^2 to describe the data [2, 3].

We also investigate some of the effects of including higher-order terms in the FRR extrapolation of lattice data. The leading contribution from the Δ -baryon, shown in Fig. 10, is also incorporated into the fit. Equation (15) becomes

$$\mu_B^{(Q)} = a_0^{B(Q)} + a_2^{B(Q)} m_\pi^2 + a_4^{B(Q)} m_\pi^4 + \chi_{B\eta'}^{(Q)} \mu_B^{(Q)} I_{\eta'} + \chi_{B\pi}^{(Q)} I_\pi + \chi_{B\pi}^{\Delta(Q)} I_{\Delta\pi}, \quad (20)$$

where, analogous to Eq. (11), the corresponding couplings are given by

$$\chi_{B\pi}^\Delta = \frac{M_N}{8\pi f_\pi^2} \beta_{B\Delta}^\pi, \quad (21)$$

and Table II. The loop integral is also modified by the fact that the intermediate baryon propagator is non-degenerate with the external state. With the mass-splitting given by Δ , Eq. (4) becomes

$$I_\pi = -\frac{4}{3\pi} \int dk \frac{(\Delta + 2\omega_k)k^4 u^2(k)}{2\omega_k^3(\Delta + \omega_k)^2}. \quad (22)$$

Given that the finite-volume corrections are negligible in the regime where the lattice QCD results lie, we illustrate the role of the Δ in FRR-EFT by taking the lat-

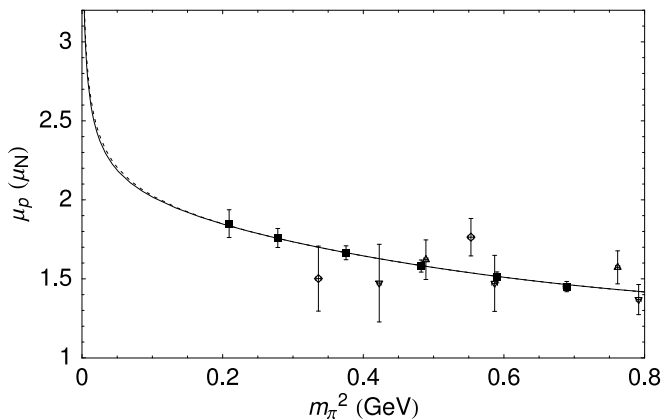


FIG. 11: The role of Δ contributions in the extrapolation of the proton magnetic moment. The solid curve displays the leading-order extrapolation of Eq. (16), without explicit decuplet contributions, as seen in Fig. 4. Equation (16) is extended to include the pion contributions with decuplet baryons in Eq. (20). The dotted curve displays the quenched fit of Eq. (20) to lattice simulation results.

tice results as an accurate representation of the infinite-volume limit and evaluate the loop integrals of Eq. (20) in the infinite volume limit.

The fit of Eq. (20) to lattice results is shown by the dotted curve of Fig. 11. The comparison with the leading order result (solid curve) shows that the effect of the decuplet on the extrapolation result is negligible. The new non-analytic behaviour introduced by an explicit inclusion of the Δ was already approximated well by the analytic terms in the expansion at leading order. Although the extrapolation shows little sensitivity to the inclusion of the Δ , it will be necessary to explicitly include this degree of freedom if one is to extract the low-energy constants to this order.

With regard to the estimation of full QCD corrections, the inclusion of the decuplet is again a small effect. With the Δ , the QCD estimate of the proton magnetic moment at the physical quark mass is increased by $0.05 \mu_N$ from the leading-order result. Although small for the proton, the inclusion of such contributions is found to be important for other baryons of the octet in the extraction of the strangeness magnetic moment of the proton [54, 55].

Finally, the prediction of the physical proton magnetic moment obtained by including the Δ contributions and

compensating for the finite lattice volume is $2.54(30) \mu_N$, where the uncertainty is statistical in origin. This result agrees well with the experimental value of $2.79 \mu_N$.

VIII. CONCLUSIONS

Quenched and physical magnetic moments are in good agreement over a large range of pion mass. Although pion effects alone are decreased in QQCD, the new behaviour introduced by the η' acts to suppress any difference.

It is commonly accepted that the dimensionally regularised expansion of the nucleon mass to $\mathcal{O}(p^4)$ is convergent to $m_\pi \sim 300$ MeV. We find that to reach similar pion masses in the DR expansion of the magnetic moment one would require knowledge of the chiral expansion to $\mathcal{O}(p^{10})$. The smooth behaviour of the lattice data, together with the series truncations of the FRR expansion indicate that although higher-order terms of DR can be individually large they effectively sum to zero in the region of interest. FRR-EFT provides an effective resummation of the chiral expansion that ensures that the slow variation of magnetic moments observed in lattice QCD arises naturally in the FRR expansion.

Finally, by estimating finite volume and quenching effects through the leading one-loop contributions of the finite-range regularized meson cloud, we obtain an excellent value for the physical magnetic moment of the proton. Combined with the previous success in describing the difference between quenched and full-QCD nucleon and Δ masses [14], these results strengthen the argument that artifacts of the quenched approximation can be accurately corrected using phenomenological methods. Ultimately, lattice QCD simulations incorporating light dynamical-quark degrees of freedom on a variety of lattice volumes are required to achieve the goal of an *ab initio* determination of nucleon properties.

Acknowledgments

We would like to thank Ian Cloet, Emily Hackett-Jones and Stewart Wright for helpful discussions. This work was supported by the Australian Research Council and by DOE contract DE-AC05-84ER40150, under which SURA operates Jefferson Laboratory.

-
- [1] D. B. Leinweber, A. W. Thomas and R. D. Young, *to appear* Phys. Rev. Lett. (2004) [arXiv:hep-lat/0302020].
 - [2] D. B. Leinweber, D. H. Lu and A. W. Thomas, Phys. Rev. D **60**, 034014 (1999) [arXiv:hep-lat/9810005].
 - [3] E. J. Hackett-Jones, D. B. Leinweber and A. W. Thomas, Phys. Lett. B **489**, 143 (2000) [arXiv:hep-lat/0004006].
 - [4] T. R. Hemmert and W. Weise, Eur. Phys. J. A **15**, 487

- (2002) [arXiv:hep-lat/0204005].
- [5] E. J. Hackett-Jones, D. B. Leinweber and A. W. Thomas, Phys. Lett. B **494**, 89 (2000) [arXiv:hep-lat/0008018].
- [6] D. B. Leinweber, A. W. Thomas and S. V. Wright, Phys. Lett. B **482**, 109 (2000) [arXiv:hep-lat/0001007].
- [7] M. Procura, T. R. Hemmert and W. Weise, Phys. Rev. D **69**, 034505 (2004) [arXiv:hep-lat/0309020].

- [8] W. Detmold *et al.*, Phys. Rev. Lett. **87**, 172001 (2001) [arXiv:hep-lat/0103006].
- [9] W. Detmold, W. Melnitchouk and A. W. Thomas, Phys. Rev. D **66**, 054501 (2002) [arXiv:hep-lat/0206001].
- [10] T. R. Hemmert, M. Procura and W. Weise, Phys. Rev. D **68**, 075009 (2003) [arXiv:hep-lat/0303002].
- [11] D. B. Leinweber, A. W. Thomas, K. Tsushima and S. V. Wright, Phys. Rev. D **64**, 094502 (2001) [arXiv:hep-lat/0104013].
- [12] R. D. Young, D. B. Leinweber and A. W. Thomas, Prog. Part. Nucl. Phys. **50**, 399 (2003) [arXiv:hep-lat/0212031].
- [13] D. B. Leinweber, A. W. Thomas, K. Tsushima and S. V. Wright, Phys. Rev. D **61**, 074502 (2000) [arXiv:hep-lat/9906027].
- [14] R. D. Young, D. B. Leinweber, A. W. Thomas and S. V. Wright, Phys. Rev. D **66**, 094507 (2002) [arXiv:hep-lat/0205017].
- [15] L. F. Li and H. Pagels, Phys. Rev. Lett. **26**, 1204 (1971).
- [16] J. F. Donoghue, B. R. Holstein and B. Borasoy, Phys. Rev. D **59**, 036002 (1999) [arXiv:hep-ph/9804281].
- [17] I. C. Cloet, D. B. Leinweber and A. W. Thomas, Phys. Lett. B **563**, 157 (2003) [arXiv:hep-lat/0302008].
- [18] M. J. Savage, Nucl. Phys. A **700**, 359 (2002) [arXiv:nucl-th/0107038].
- [19] D. B. Leinweber, Phys. Rev. D **69**, 014005 (2004) [arXiv:hep-lat/0211017].
- [20] S. R. Sharpe, Phys. Rev. D **46**, 3146 (1992) [arXiv:hep-lat/9205020].
- [21] C. W. Bernard and M. F. L. Golterman, Phys. Rev. D **46**, 853 (1992) [arXiv:hep-lat/9204007].
- [22] D. B. Leinweber, A. W. Thomas and R. D. Young, Phys. Rev. Lett. **86**, 5011 (2001) [arXiv:hep-ph/0101211].
- [23] M. Gockeler *et al.* [QCDSF Collaboration], arXiv:hep-lat/0303019.
- [24] J. M. Zanotti *et al.*, Nucl. Phys. Proc. Suppl. **128**, 233 (2004) [arXiv:hep-lat/0401029].
- [25] J. M. Zanotti, D. B. Leinweber, A. G. Williams and J. B. Zhang, Nucl. Phys. Proc. Suppl. **129**, 287 (2004) [arXiv:hep-lat/0309186].
- [26] D. B. Leinweber, R. M. Woloshyn and T. Draper, Phys. Rev. D **43**, 1659 (1991).
- [27] S. J. Dong, K. F. Liu and A. G. Williams, Phys. Rev. D **58**, 074504 (1998) [arXiv:hep-ph/9712483].
- [28] R. Lewis, W. Wilcox and R. M. Woloshyn, Phys. Rev. D **67**, 013003 (2003) [arXiv:hep-ph/0210064].
- [29] M. Luscher *et al.*, Nucl. Phys. B **491**, 323 (1997) [arXiv:hep-lat/9609035].
- [30] J. M. Zanotti *et al.* [CSSM Lattice Collaboration], Phys. Rev. D **65**, 074507 (2002) [arXiv:hep-lat/0110216].
- [31] D. B. Leinweber and A. W. Thomas, Phys. Rev. D **62**, 074505 (2000) [arXiv:hep-lat/9912052].
- [32] J. D. Ashley, D. B. Leinweber, A. W. Thomas and R. D. Young, arXiv:hep-lat/0308024.
- [33] V. V. Flambaum, D. B. Leinweber, A. W. Thomas and R. D. Young, *to appear* Phys. Rev. D (2004) [arXiv:hep-ph/0402098].
- [34] R. D. Young, D. B. Leinweber and A. W. Thomas, Nucl. Phys. Proc. Suppl. **128**, 227 (2004) [arXiv:hep-lat/0311038].
- [35] R. D. Young, D. B. Leinweber and A. W. Thomas, Nucl. Phys. Proc. Suppl. **129-130C**, 290 (2004) [arXiv:hep-lat/0309187].
- [36] D. B. Leinweber *et al.*, [arXiv:nucl-th/0308083].
- [37] J. Gasser and H. Leutwyler, Nucl. Phys. B **307**, 763 (1988).
- [38] A. Ali Khan *et al.* [QCDSF-UKQCD Collaboration], arXiv:hep-lat/0312030.
- [39] S. R. Beane, arXiv:hep-lat/0403015.
- [40] B. Orth, T. Lippert and K. Schilling, Nucl. Phys. Proc. Suppl. **129-130**, 173 (2004) [arXiv:hep-lat/0309085].
- [41] G. Rupak and N. Shores, Phys. Rev. D **66**, 054503 (2002) [arXiv:hep-lat/0201019].
- [42] O. Bar, G. Rupak and N. Shores, Phys. Rev. D **67**, 114505 (2003) [arXiv:hep-lat/0210050].
- [43] S. Aoki, Phys. Rev. D **68**, 054508 (2003) [arXiv:hep-lat/0306027].
- [44] M. Luscher, S. Sint, R. Sommer and P. Weisz, Nucl. Phys. **B478** (1996) 365 [hep-lat/9605038]; M. Luscher, S. Sint, R. Sommer, P. Weisz and U. Wolff, Nucl. Phys. **B491** (1997) 323, 344 [hep-lat/9609035].
- [45] R. Narayanan and H. Neuberger, Phys. Lett. B **302**, 62 (1993) [arXiv:hep-lat/9212019]; *ibid.* Nucl. Phys. B **412**, 574 (1994) [arXiv:hep-lat/9307006]; *ibid.* Phys. Rev. Lett. **71**, 3251 (1993) [arXiv:hep-lat/9308011]; *ibid.* Nucl. Phys. B **443**, 305 (1995) [arXiv:hep-th/9411108].
- [46] J. M. Zanotti, B. G. Lasscock, D. B. Leinweber and A. G. Williams, arXiv:hep-lat/0405015.
- [47] R. G. Edwards, U. M. Heller and T. R. Klassen, Phys. Rev. Lett. **80**, 3448 (1998) [hep-lat/9711052].
- [48] S. J. Dong, F. X. Lee, K. F. Liu and J. B. Zhang, Phys. Rev. Lett. **85**, 5051 (2000) [arXiv:hep-lat/0006004].
- [49] M. Luscher and P. Weisz, Commun. Math. Phys. **97**, 59 (1985) [Erratum-*ibid.* **98**, 433 (1985)].
- [50] R. G. Edwards, U. M. Heller and T. R. Klassen, Nucl. Phys. B **517**, 377 (1998) [arXiv:hep-lat/9711003].
- [51] R. E. Stuckey and M. C. Birse, J. Phys. G **23**, 29 (1997) [arXiv:hep-ph/9602312].
- [52] S. V. Wright, *PhD Thesis*, University of Adelaide (2002).
- [53] C. Bernard *et al.*, Nucl. Phys. Proc. Suppl. **119**, 170 (2003) [arXiv:hep-lat/0209086].
- [54] D. B. Leinweber *et al.*, Nucl. Phys. Proc. Suppl. **128**, 132 (2004) [arXiv:hep-lat/0406003].
- [55] D. B. Leinweber *et al.*, arXiv:hep-lat/0406002.